ACS APPLIED MATERIALS & INTERFACES

LETTER

www.acsami.org

Interface Architecture Determined Electrocatalytic Activity of Pt on Vertically Oriented TiO_2 Nanotubes

Robert E. Rettew,[†] Nageh K. Allam,[‡,§] and Faisal M. Alamgir*[,†]

[†]School of Materials Science and Engineering and [‡]Laser Dynamics Laboratory, School of Chemistry and Biochemistry, Georgia Institute of Technology, Atlanta, Georgia 30332, United States

ABSTRACT: The surface atomic structure and chemical state of Pt is consequential in a variety of surface-intensive devices. Herein we present the direct interrelationship between the growth scheme of Pt films, the resulting atomic and electronic structure of Pt species, and the consequent activity for methanol electro-oxidation in Pt/TiO_2 nanotube hybrid electrodes. X-ray photoelectron spectroscopy (XPS) and X-ray absorption spectroscopy (XAS) measurements were performed to relate the observed electrocatalytic activity to the oxidation state and the atomic structure of the deposited Pt species. The atomic structure as well as the oxidation state of the deposited Pt was found to depend on the pretreatment of the TiO_2 nanotube surfaces with electrodeposited Cu. Pt growth through Cu replacement increases Pt dispersion, and a separation of surface Pt atoms beyond a threshold distance from the TiO_2 substrate renders them metallic, rather than cationic. The increased dispersion and the metallic character of Pt results in strongly enhanced electrocatalytic activity toward methanol oxidation. This study points to a general phenomenon whereby the growth scheme and the substrate-to-surface-Pt distance dictates the chemical state of the surface Pt atoms, and thereby, the performance of Pt-based surface-intensive devices.

KEYWORDS: TiO_2 nanotubes, Pt, Cu replacement, methanol oxidation, fuel cell, XPS, XAS, cationic Pt

INTRODUCTION

It is widely recognized that the development of fuel cells that directly utilize renewable liquid fuels will require the design and optimization of new catalytic materials as well as new protocols that involve the modification of the currently used materials.[1,2] One critical component in these systems is the catalyst−supporting material. As the commonly used carbon supporting materials suffer from the weak dispersion of the catalyst on their surfaces as well as its poor loading capacity, a plethora of efforts have been devoted toward the search for better catalyst supporting materials that tolerate these limitations. In this regard, titanium dioxide is an attractive material as a support for metallic electrocatalysts because of the strong nature of the metal−support interaction.[3] Traditional fabrication processing routes of TiO_2 nanoarchitectures include the thermal oxidation of titanium metal at very high temperatures, template assembly, and colloidal methods.[4] However, high-temperature processes usually limit control over the fine interfacial features of TiO_2 films which significantly affect their properties.[5] Templated and colloidal synthesis routes require subsequent careful assembly onto conductive substrates as needed for device integration. Further, the resultant nanomaterials are prone to aggregation when the templates are etched away.[4] It is only through recent development of metal oxide etching processes that highly ordered TiO_2 nanotubular structures (TNT) were produced directly on Ti foil, resulting in a structure that has all of the morphological benefits of traditional TNT while also enjoying the advantages of vertically oriented nanotubes with tunable height and diameter.[6−11] Furthermore, this synthesis protocol retains a metal back foil as an efficient electrical contact, which is very useful for electrocatalysis.

As the Pt/TiO_2 system is stable over a wide range of pH values,[12] work has been conducted studying traditionally grown Pt-modified TiO_2 for applications including the methanol electro-oxidation reaction, among others.[13,14] Of particular interest is the work by Iida and Igarashi indicating that the Pt-TiO_2 support interaction can be employed to weaken the Pt-CO poisoning interaction.[15] However, it is still a challenge to achieve a high degree of dispersion of Pt over TiO_2 surfaces as well as increasing the catalyst load.

As with the design of an efficient catalytic system, rational design of beneficial metal−support interactions requires fundamental knowledge of the structure and the chemical nature of the grown metal films on the support. Therefore, this study is aimed at exploring galvanic replacement of a Cu precursor to improve the dispersion and loading of Pt on TiO_2 nanotube surfaces as well as exploring the fundamental structure−property relationships of Pt-TiO_2 hybrid surfaces. The application of these materials is then demonstrated for methanol electro-oxidation. Specifically, we investigate transitions in the local atomic and electronic structure of ultrathin Pt films as a function of the method and the extent of film growth. We further investigate the relationship between the atomic and electronic structure of Pt to the activity of the resulting Pt-TiO_2 toward methanol oxidation. We believe this work to be very important for both electrocatalytic and photocatalytic applications and hope that this study will open a new vista to explore more metal-TiO_2 combinations for a diversity of various applications.

EXPERIMENTAL SECTION

Fabrication of Hybrid Electrodes. Prior to anodization, titanium foil samples were ultrasonically cleaned with acetone followed

Received: December 21, 2010
Accepted: January 24, 2011
Published: January 26, 2011

by a deionized (D.I.) water rinse. The anodization was performed in a two-electrode electrochemical cell with titanium foil as the working electrode and platinum foil as the counter electrode at room temperature (approximately 22 °C) at 20 V for 7 h in an aqueous electrolyte containing 0.2 M NH_4F and 0.1 M H_3PO_4. An Agilent E3612A DC power supply was used for potentiostatic anodization. Afterward, the samples were rinsed thoroughly with deionized water and isopropyl alcohol and then dried under nitrogen stream. Samples were not annealed, resulting in amorphous TNT structures. Pt deposits were formed by dipping in 1 mM H_2PtCl_6 at open circuit for ten minutes with and without Cu precursor film. The Cu precursor, when present, was potentiostatically grown at −0.5 V vs Ag/AgCl from a 10 mM $CuSO_4$/50 mM H_2SO_4 solution for either 1 min or for 5 min.

Characterization of the Fabricated Electrodes. The fabricated electrodes were examined using a Zeiss SEM Ultra60 field emission scanning electron microscope (FESEM). X-ray photoelectron spectroscopy (XPS) experiments were performed on the TiO_2 films using a Thermo Scientific K-alpha XPS system where the binding energy of all samples were calibrated to that of a Au reference sample. Pt L_3-edge EXAFS measurements were conducted at beamline X23A2 at the National Synchrotron Light Source (NSLS), Brookhaven National Laboratory. Measurements were made in glancing incidence fluorescence mode. The k-space data was truncated by a standard Hanning function before Fourier transforming to real space.

Electrochemical Measurements. The electrodes were electrochemically characterized by cyclic voltammetry (CV) using a Pine WaveNow potentiostat in a three-electrode electrochemical cell with Pt wire as a counter electrode and a Ag/AgCl reference electrode. CV experiments were performed in 1 M H_2SO_4 solution with 1 M CH_3OH at a scan rate of 50 mV/s. Current densities are plotted as a function of Ti foil surface area before TNT growth.

RESULTS

Samples were fabricated by exposing the TNT (3.7 μm in length and 90 nm in diameter) electrode to Pt^{4+} solutions with and without the presence of Cu precursors on the surface. The redox reaction of Pt^{4+} with Cu^0 allowed Pt to grow in a highly dispersed manner on the surface at the expense of the Cu, which is partially dissolved. This method resulted in morphologies with highly dispersed platinum coexisting with Cu/Pt. Scheme 1 portrays these microstructures in representative form, with Cu (blue) and Pt (red) deposits. The scheme illustrates the dispersion of small Pt nuclei that results from spontaneous Pt growth without Cu precursor. The increased dispersion which arises as a result of Cu-mediated growth is shown as a continuous red film coexisting with on-top Pt and Cu nuclei. 2D profile views of the scheme are provided to clarify that residual Cu is present both as an underlying film and as on-top nuclei. Cu-mediated growth is preferable to the direct galvanic growth of Pt, which would result in larger Pt nuclei. This type of redox replacement has been performed in the past for noble metals replacing Cu,[16,17] Ni,[18,19] and other metals on various substrates.

Figure 1 shows FESEM top-view images of the fabricated electrodes. Figure 1A shows the as-grown TNT where highly ordered hexagonal close packed cells can be seen. Figure 1B shows the nanotubes after a 10 min immersion in the Pt solution (1 mM H_2PtCl_6) without any Cu precursor. Note the light-colored deposits nucleating around the rims of the tubes. Cu deposition for 1 min followed by the same 10 min immersion in Pt solution (Figure 1C) resulted in coarsening of the tube walls due to thicker intratubular deposits as well as some supra-tubular nuclei 100−200 nm in size. Increasing the Cu deposition to

Scheme 1. Cartoon Showing 3D and Profile Representations of TNT's with Spontaneous Pt Growth and Cu-Mediated Pt Growth; Note That Pt Deposits (red) Are Grown on Both Cu (blue) and TiO_2 Sites in the Cu-Mediated Case

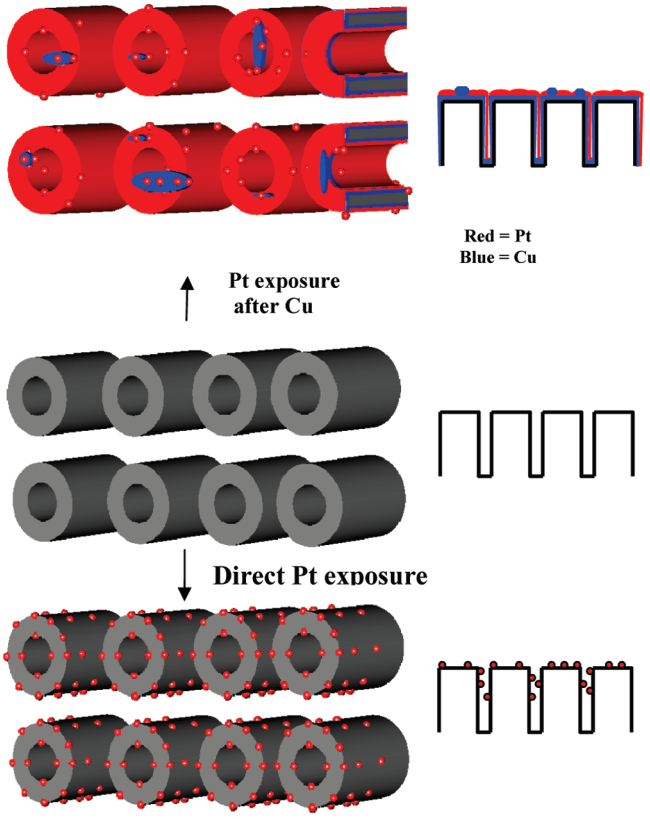

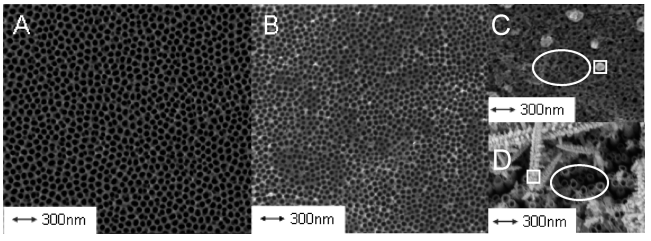

Figure 1. FESEM top view image of the TiO_2 electrode: (A) as-prepared, (B) after 10 min Pt exposure, (C) 1 min Cu growth replaced by 10 min H_2PtCl_6 exposure, and (D) after 5 min Cu growth exposed to 10 min H_2PtCl_6. EDS spectra were taken on tubular and supra-Cu regions as represented by the ovals and squares, respectively.

5 min, followed once again by 10 min Pt solution immersion, (Figure 1D) appear to coarsen the TNT tubes further and increase the size of the supra-tubular deposits. Localized energy dispersive X-ray spectroscopy (EDS) analysis of the Pt-TiO_2 sample grown via 1 min Cu precursor indicated that the supra-tubular nuclei contained both Pt and Cu in a 2:1 atomic ratio, on average, while the intratubular deposits showed a ratio of 5:1. For the 5 min Cu growth, EDS indicated approximate Pt:Cu ratios of 4:1 on the nuclei and 1:1 on the tube sites.

To further investigate the surface composition and chemical state of the fabricated electrodes, we performed XPS analyses. Figure 2 shows the Pt 4f XPS spectra for the different Pt@TNT

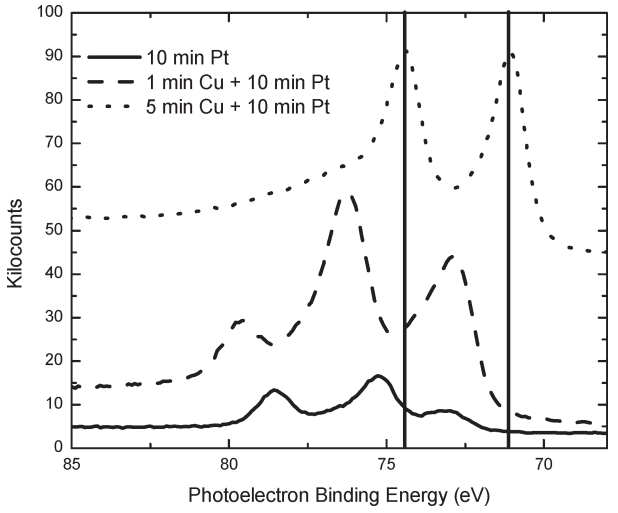

Figure 2. XPS spectra of platinized TiO_2 nanotube electrodes. Lines indicate location of peaks for Pt reference foil.

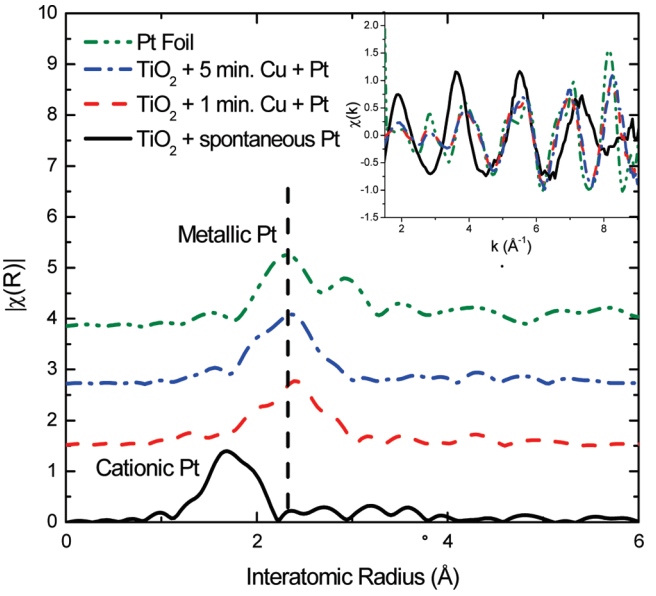

Figure 3. Fourier transform of Pt L3-edge EXAFS data of TiO_2 samples with and without varying Pt treatment methods. Inset shows k-space spectra before Fourier transform.

electrodes. Lines at 71.1 eV and 74.4 eV indicate the location of Pt foil reference peaks. The spectra for the spontaneously grown Pt and the Pt after a 1 min Cu treatment are positively shifted from that for the 5 min Cu treated electrode, indicating that Pt exists in a cationic state. Specifically, the presence of a peak pair at 72.8 and 76.2 eV corresponds to $4f_{7/2}$ and $4f_{5/2}$ photoemission from Pt^{2+} species, while pairs in the ranges of 75.1−76.1 eV and 78.4−79.5 eV correspond to respective pairs from the Pt^{4+} species. The sample modified with electrodeposited Cu for 1 min has a higher proportion of Pt^{2+} compared to the spontaneously grown sample. However, the sample modified with a 5 min Cu deposition does not show significant signs of cationic species, exhibiting only one pair of peaks (71.1 and 74.4 eV) indicative of metallic character. It is apparent that the chemical identity of Pt varies with growth treatment. However, XPS does not provide the atomic structure within the Pt deposits. Therefore, to characterize structure of the deposits, X-ray absorption measurements were performed.

Figure 3 depicts the magnitude of the real-space modified atomic radial distribution function, $|\chi(r)|$, of collected Pt L3-edge EXAFS data for 3 treatments of Pt on TiO_2 tubes, and a Pt reference. The inset provides the corresponding $\chi(k)$ functions. By examining the location of the lowest-coordination peak in real space, it can be seen that spontaneously grown Pt is nonmetallic in nature, with its first coordination shell located at 1.8 Å (phase corrections not corrected for). Deposits grown via Cu precursors exhibit a first coordination shell characteristic of the metal reference, located at 2.4 Å.

To evaluate the electrocatalytic activity of the fabricated electrodes, we carried out cyclic voltammetric (CV) studies in 1 M sulfuric acid with 1 M methanol, see Figure 4A. Note that the methanol electro-oxidation currents were seen during the forward sweep at 0.75 V and during the reverse sweep at 0.52 V for all samples treated with Pt, with higher currents recorded for the samples premodified with Cu layer. During the anodic scan, the current increases due to dehydrogenation of methanol followed by the oxidation of absorbed methanol residues, while in the cathodic scan, the reoxidation of the residues is occurring. It is important to note that the cyclic voltammogram for the Pt-dipped TNT without any Cu modification is shown in 5x scale to aid readability. Figure 4B displays the peak currents after normalization to integrated Pt XPS peak area, which is proportional to the surface loading of Pt. The high electrocatalytic activity of Pt/TiO_2 hybrid electrodes can be mainly attributed to the remarkably active platinum sites on the TiO_2 nanotube matrix. As amorphous titania nanotubes have many OH groups on their surfaces,[20,21] it is possible that these OH moieties help in the conversion of CO poisoning species into CO_2, leaving the active sites on Pt clean for further electrocatalytic reactions in a similar way to that which Ru is doing in the commercially used Pt−Ru/C catalysts. In addition, the strong metal−support interaction could be another reason for the observed enhanced electrocatalytic activity of methanol oxidation at Pt/TiO_2 hybrid electrodes.

DISCUSSION

It is apparent that the dipping of the TiO_2 nanotube electrode in H_2PtCl_6 solution resulted in the formation of intratube deposits of Pt species (Figure 1A). This spontaneous growth likely occurs through the immobilization of $PtCl_6^{2-}$ at the exposed OH sites on the TiO_2 surface. This would explain the higher oxidation state for the spontaneously grown Pt species as evidenced by XPS analysis (Figure 2). This interpretation is further consistent with the EXAFS data for spontaneous growth, showing a lower first coordination shell distance of R=1.8 Å compared to the 2.4 Å coordination shell exhibited by the Pt deposits resulting from Cu replacement (Figure.3). The presence of spontaneously grown Pt in the cationic form has many implications on its catalytic properties. For example, Hayden et al. showed very recently that the photocatalytic activity of the system CdS/TiO_2 is superior to the system CdS/TiO_2/Pt when used to photoelectrochemically disinfect E-coli.[6] On the other hand, Iwata et al. studied the charge carrier dynamics in TiO_2 and Pt/TiO_2 materials and found very fast electron decay kinetics in the Pt/TiO_2 system relative to the pure TiO_2 system.[22] They related this fast decay kinetics to the trapping of free electrons. However, in both cases, no explanation was given based on the electronic structure of Pt when attached to TiO_2. Our present results can clearly indicate the possibility of electron traps at the Pt cationic sites indicating that Pt cations can act as an electron

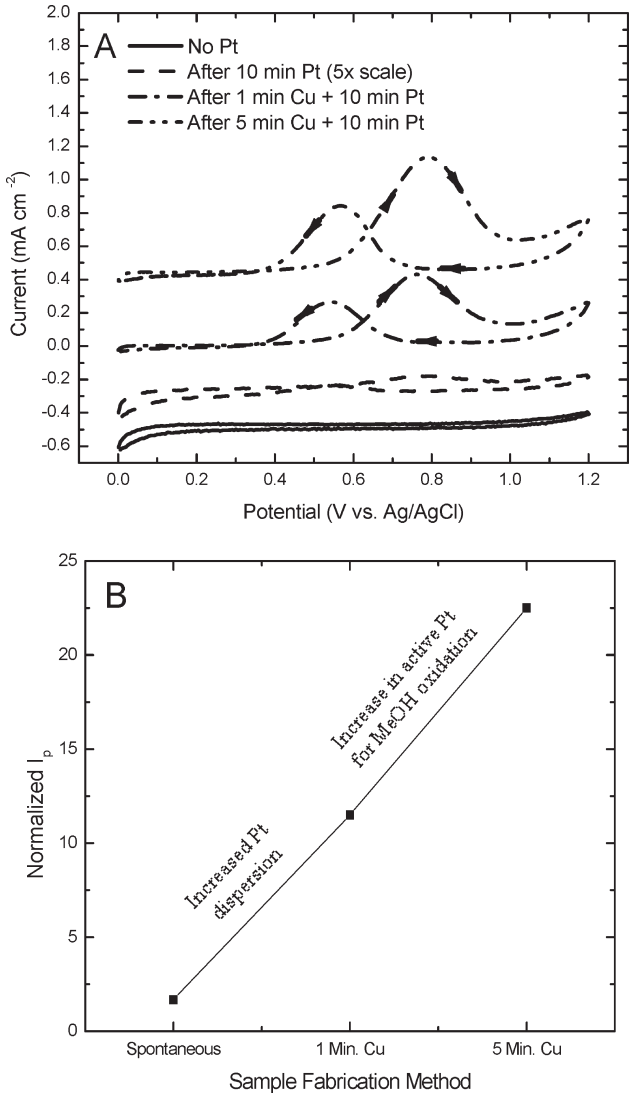

Figure 4. (A) Cyclic voltammograms of the electrodes in 1 M H_2SO_4 + 1 M Methanol. (B) Forward peak current (I_P) values normalized to Pt surface loading as measured by XPS.

sink. This finding is very important for the design of photoactive material systems.

When Cu precursor is used, the intratubular deposits are accompanied by some supra-tubular deposits, but in terms of Pt surface area, the intratubular deposits dominate. EDS analysis shows that, even in the case of lower precursor content, 10 min are insufficient for Pt ions to replace all the intratube Cu. Increasing the amount of Cu precursor deposition should, then, result in topical Pt that is further away from the TiO_2 substrate and result in diminishing Pt-TiO_2 metal−support interaction. The assertion is supported by the XPS data when comparing the Pt oxidation states between the samples. When surface Pt is relatively closer to the support (1 min. Cu deposit case) it remains cationic while the Pt which is further from the support (5 min deposit case) is metallic. We suggest that in the former case the underlying TiO_2 continues to immobilize $PtCl_6^{2-}$ on the surface in much the same way as with the spontaneous Pt deposition scheme. In the latter case, the surface Pt is beyond the threshold Pt-TiO_2 metal−support interaction distance. At the same time the net atomic structure of Pt, as seen by EXAFS (Figure 3), for both cases where it is grown through Cu replacement retains the FCC-like structure characteristic of metallic Pt. This suggests that while the Pt deposits resulting from 1 min Cu doses arrange themselves as Pt metal, their surface chemistry is still dominated by an oxidic character (as seen by XPS).

Finally, by normalizing the methanol oxidation currents to the integrated XPS area for Pt, we get a measure of the reactivity per unit Pt present on the surface (Figure 4B). This allows us to relate performance to the local environment and oxidation state of the as-grown deposits. While Cu replacement increases Pt dispersion, growth beyond a threshold film thickness ensures a predominance of metallic, rather than cationic, Pt on the surface. We see clearly that Pt grown beyond this threshold metal−support interaction distance retains metallic character and exhibits enhanced electrocatalytic activity toward methanol oxidation.

SUMMARY AND CONCLUSIONS

We demonstrated the platinization of titanium-foil-supported, highly ordered, vertically oriented titania nanotube arrays (TNT) by spontaneous growth and galvanic replacement of a Cu precursor layer. We have tracked, using SEM, the formation increased intratubular metal deposition. Spontaneously grown Pt exhibits cationic local structure, limited dispersion and relatively low activity for methanol electro-oxidation. With the predeposition of Cu, the dispersion of surface Pt is significantly increased. Increasing the metal−support distance, by increasing the thickness of the Cu predeposited layer, the surface Pt is rendered metallic Pt rather than cationic, which further increases the activity of Pt for methanol electro-oxidation.

AUTHOR INFORMATION

Corresponding Author

*faisal.alamgir@mse.gatech.edu.

Present Addresses

§Department of Electrical Engineering and Computer Science, Massachusetts Institute of Technology, Cambridge, MA 02139. E-mail: Nageh.Allam@gmail.com.

ACKNOWLEDGMENT

The authors acknowledge technical support from Bruce Ravel at beamline X23A2 of the NSLS. We thank the Synchrotron Catalysis Consortium for travel support to the NSLS. NKA would like to thank the Department of Energy (DE-FG02-97ER14799) and the RAK-CAM Foundation for the support of this work.

REFERENCES

(1) Sammes, N., *Fuel Cell Technology.*: Springer: New York, 2006; p 298.
(2) Tawfik, H.; Hung, Y.; Mahajan, D. *J. Power Sources* **2007**, *163*, 755.
(3) Tauster, S. J.; Fung, S. C.; Garten, R. L. *J. Am. Chem. Soc.* **1978**, *100*, 170.
(4) Chen, X.; Mao, S. S. *Chem. Rev.* **2007**, *107*, 2891–2959.
(5) Allam, N. K.; Shankar, K.; Grimes, C. A. *Adv. Mater.* **2008**, *20*, 3942.
(6) Hayden, S. C.; Allam, N. K.; El-Sayed, M. A. *J. Am. Chem. Soc.* **2010**, *132*, 14406.
(7) Allam, N. K.; Grimes, C. A. *Langmuir* **2009**, *25*, 7234.
(8) Allam, N. K.; El-Sayed, M. A. *J. Phys. Chem. C* **2010**, *114*, 12024.
(9) Allam, N. K.; Alamgir, F.; El-Sayed, M. A. *ACS Nano* **2010** *4*, 5819.

(10) Allam, N. K.; Shankar, K.; Grimes, C. A. *J. Mater. Chem.* **2008**, *18*, 2341.
(11) Allam, N. K.; Grimes, C. A. *Sol. Energy Mater. Sol. Cells* **2008**, *92*, 1468.
(12) Shim, J.; Lee, C. R.; Lee, H. K.; Lee, J. S.; Cairns, E. J. *J. Power Sources* **2001**, *102*, 172.
(13) Mandelbaum, P. A.; Regazzoni, A. E.; Blesa, M. A.; Bilmes, S. A. *J.Phys. Chem.B* **1999**, *103*, 5505.
(14) He, D.; Yang, L.; Kuang, S.; Cai, Q. *Electrochem. Commun.* **2007**, *9*, 2467.
(15) Iida, H.; Igarashi, A. *Appl. Catal., A* **2006**, *298*, 152.
(16) Kim, Y. G.; Kim, J. Y.; Vairavapandian, D.; Stickney, J. L. *J. Phys. Chem. B* **2006**, *110*, 17998.
(17) Sayed, S. Y.; Buriak, J. M. *ACS Appl. Mater. Interfaces* **2010**, *2*, 3515.
(18) Rettew, R. E.; Guthrie, J. W.; Alamgir, F. M. *J. Electrochem. Soc.* **2009**, *156*, D513.
(19) Tegou, A.; Armyanov, S.; Valova, E.; Steenhaut, O.; Hubin, A.; Kokkinidis, G.; Sotiropoulos, S. *J. Electroanal. Chem.* **2009**, *634*, 104.
(20) Grimes, C. A., Mor, G. K. *TiO_2 Nanotube Arrays: Synthesis, Properties, and Applications*; Springer: Norwell, MA, 2009.
(21) Allam, N. K.; Grimes, C. A. *J. Phys. Chem. C* **2007**, *111*, 13028.
(22) Iwata, K.; Takaya, T.; Hamaguchi, H.; Yamakata, A.; Ishibashi, T.; Onishi, H.; Kuroda, H. *J. Phys. Chem. B* **2004**, *108*, 20233.